How does an airfoil’s maximum thickness affect the lift versus drag produced at various angles of attack?

Mina Mikhail

Table of Contents

Background Information

Airfoils

An airfoil is the cross-section of an airplane wing constructed in a way that air flows around it to produce useful motion. The chord length is the straight-line distance between the leading and trailing edges of an airfoil. The camber of an airfoil specifies the curvature of the airfoil; the mean camber lies halfway between the upper and lower surfaces of an airfoil. The angle of attack is the angle relative to the oncoming airflow. (Benson, 2021)

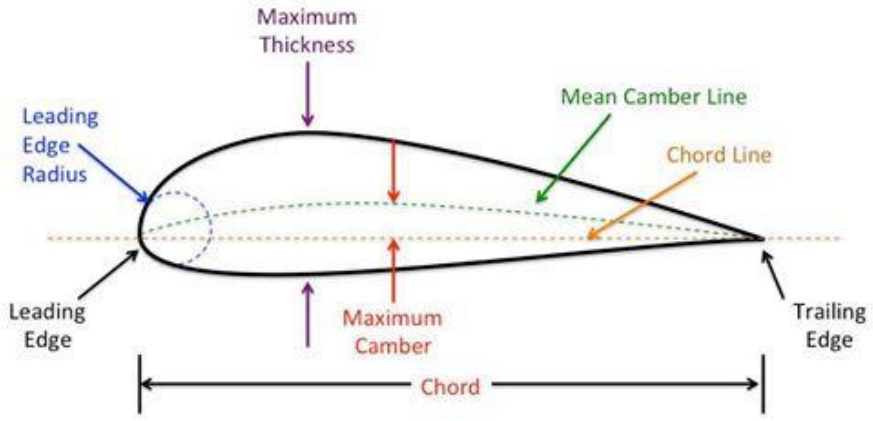

Figure 1: (Abdallah et al., 2015)

Airfoils can be identified by a four-digit NACA number. The first digit defines the maximum camber as a percentage of the chord length. The second describes the position of maximum camber from the leading edge as tenths of the chord. The last two digits define the maximum thickness as a percentage of the chord. (Stanford, 2004)

Theories of Lift

Newton's Third Law of Motion

Newton's Third Law of Motion states that for every action there is a reaction of equal magnitude and opposite direction. The shape of an airfoil along with the angle of attack allows it to deflect an oncoming fluid downward, therefore producing a force in the opposite direction which is the lift force. (Science Learning Hub, 2021)

Bernoulli's Principle

Bernoulli's Principle provides a relationship between the static pressure and dynamic pressure within a fluid flow. Static pressure is the force exerted per area by gas molecules that collide with a surface (Hall, 2021). Dynamic pressure is the kinetic energy per unit of volume of the flow (Cole, 2015). Bernoulli's equation relates them as follows:

$$static\ pressure + dynamic\ pressure = p_s + \frac{rv^2}{2} = constant \quad \textit{Equation 1}$$

Where p_s is the static pressure and the dynamic pressure is equal to one half the density of the fluid, r, times the velocity of the fluid, v, squared. This equation assumes that the fluid is incompressible. Since this procedure will use low airspeeds, much less than the speed of sound, the flow will be considered incompressible. (Hall, 2021)

In the case of an airfoil, the air on the upper surface accelerates air to a greater speed than that on the bottom (Fairman, 1996). As such, the dynamic pressure increases and by Bernoulli's equation the static pressure must decrease. There exists a pressure deferential between the upper and lower surfaces which is the lift force. (Hall, 2021)

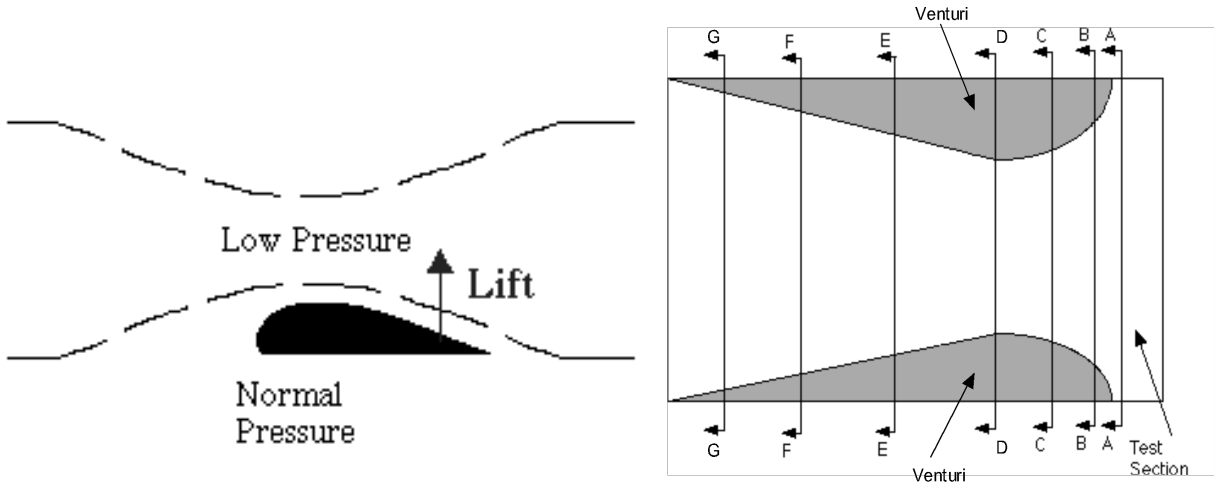

Figure 2: Airfoil acting as a venturi (Fairman, 1996)

To see why an airfoil accelerates air molecules on its upper surface, it can be approximated to half of a venturi tube. We can thus use the Continuity Equation which is typically applied to venturis:

$$A * v = constant \qquad \textit{Equation 2}$$

A is the cross-sectional area within a venturi and v is the airspeed of that particular section. Since the product of the two remains constant, as the cross-sectional area decreases or the venturi's area enlarges, the airspeed of that section increases. If an airfoil is thought of as a venturi, it becomes clear why the airspeed increases for a more pronounced curvature. (NASA, n.d.; Fairman, 1996)

Drag

Induced drag is a by-product of lift. At the wing-tips of an airfoil, the higher pressure air below the wing spills into the lower pressure air above the wing, forming wingtip vortices. These

vortices exert a downward force on the airfoil. This causes a component of the lift force to be inclined slightly backward. (SKYbrary, n.d.)

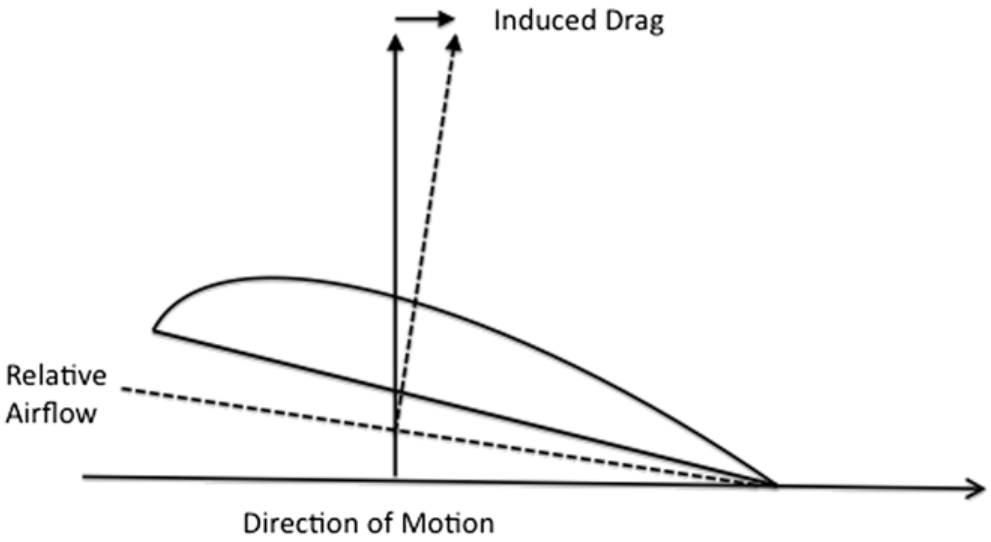

Figure 3: Induced drag as a by-product of lift (Rez, 2018)

Another type of drag is parasitic drag. This is the drag not caused by lift, including shape resistance, skin friction, and interference. (Boyne & Vance, 2025)

Lift and Drag Equations

The lift and drag equations are as follows:

$$L = \frac{1}{2} * C_l * p * v^2 * A \qquad \textit{Equation 3}$$

$$D = \frac{1}{2} * C_d * p * v^2 * A \qquad \textit{Equation 4}$$

Where C_l and C_d are the coefficients of lift and drag, p is the air density, v is the velocity, and A is the wing area. The coefficients of lift and drag must be determined experimentally. (Dasilva, 2024)

Lift to Drag Ratio

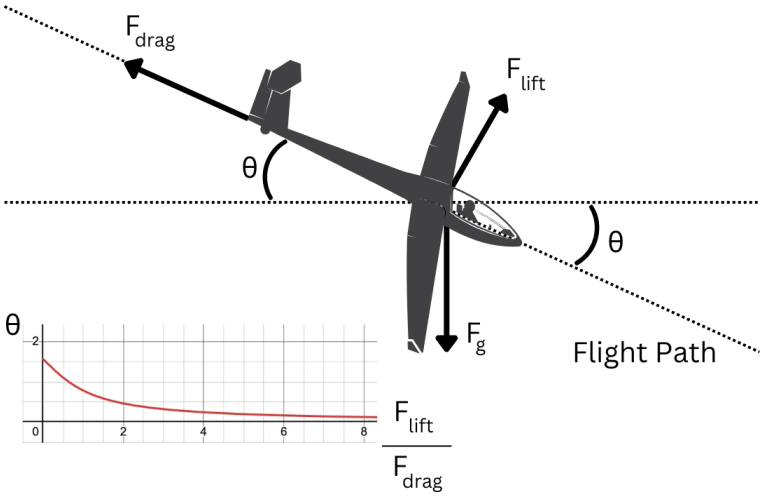

Figure 4: Forces acting on an aircraft

$$F_{lift} \sin\theta = F_{drag} \cos\theta$$

$$\cot\theta = \frac{F_{lift}}{F_{drag}}$$

The lift force to drag force ratio can be used to solve for the flight path angle θ. (Dasilva, 2024) Restricting the flight angle between 0° and 90°, it becomes clear that a higher lift to drag ratio provides a shallower flight path.

Angle of Attack

At the surface of an airfoil, the molecules on the surface stick to it. These molecules slow down the molecules above the surface. Moving away from the airfoil's surface, fewer collisions are affected by the object's surface. This thin layer from which the velocity changes from zero at the

surface to the airflow's velocity away from the surface is called the boundary layer. (Benson, n.d.)

External flow reacts as to the edge of boundary layer as it would to a physical surface. Therefore, the boundary layer gives an airfoil an effective shape which is different than its physical one. At high angles of attack, the boundary layer separates from the airfoil surface creating an effective shape that is very different than the real one. At this point the boundary layer becomes turbulent. (Benson, n.d.)

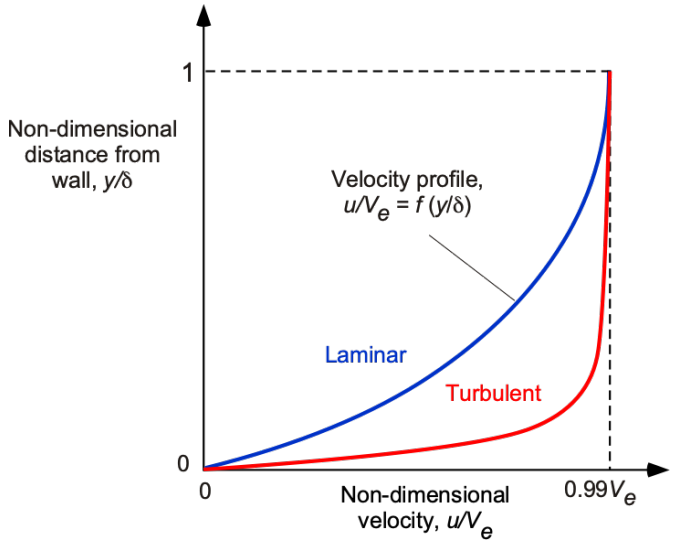

Figure 5: Velocity in boundary layer - laminar vs turbulent

Figure 5 shows how detrimental turbulent flow can be to the boundary layer. δ is the boundary layer's thickness and y is the distance from the surface. V_e is the external flow velocity, the velocity of air above the boundary layer. u is the velocity of the flow within a particular point in the boundary layer. The graph shows that with turbulent flow, the velocity within the boundary

layer is much lower and has an abrupt increase in reaching the external flow velocity. (Leishman, 2022)

The amount of lift produced by an airfoil typically increases with angle of attack but reaches a maximum at the stall angle. At this angle, flow separation has progressed to the point where it produces a loss of lift – the flow becomes turbulent. (Leishman, 2022) This aligns with the two theories of lift presented earlier: a higher angle of attack has a more pronounced curvature deflecting more air downwards which satisfies Newton's Third Law; it also produces a greater pressure gradient. If the flow became turbulent however, smaller airspeeds within the boundary layer would lead to a smaller pressure deferential according to Bernoulli's equation and less air would be deflected downward also leading to a smaller lift force according to Newton's Third Law.

The drag force produced by an airfoil increases as angle of attack does. Therefore, since as angle of attack increases both lift and drag, the lift force can be compared with the drag force to determine the max lift-drag ratio. (SimScale, 2023). As explained, this is important as it in turn determines the flight path angle.

Hypothesis

Assuming that an airfoil approximates a venturi, a thicker airfoil produces a more pronounced camber. It then constricts the theoretical area above it, and from *Equation 2* it thus requires a faster airspeed. By Bernoulli's equation, *Equation 1*, a higher airspeed leads to lower air pressure which correlates to a higher lift force. Therefore, a greater airfoil thickness will likely produce a higher lift force at every angle of attack.

Parasitic drag is likely to increase with a higher airfoil thickness because it creates a body with a larger surface area. Induced drag is directly proportional to the lift force squared where AR is the aspect ratio, the square of the wing length divided by the wing area; and e is the efficiency factor which is dependent on the wing shape. For rectangular wings, the efficiency factor is 0.7. (Dasilva, 2023)

$$C_{di} = \frac{Cl^2}{\pi * AR * e} \quad \textit{Equation 5}$$

AR and e are constant for this procedure, so if lift increases for thicker airfoils, induced drag will as well. Since both parasitic and induced drag are expected to increase, the total drag force comprised of both will increase as well for thicker airfoils.

Experimentation

Variables

Table 1: Procedure Variables

Type	**Variable**	**Reasoning**
Independent	The maximum thickness of an airfoil, measured as a percentage of the chord.	The thickness percentages of the chord that will be analyzed are 6%, 9%, 12%, 15%, 18%, 21% or NACA numbers of 5306, 5309, 5312, 5315, 5318, 5321.

		Airfoil thicknesses used vary depending on the application, so the minimum and maximum values that the setup could handle were taken.
Dependent	Raw: The lift force produced measured in grams.	Both the lift and drag forces were measured as the upward force produced on an initially zeroed balance. At every angle of attack, 5 data points were recorded for the lift and drag forces. While forces are typically measured in Newtons, it would require a simple scale factor conversion that would affect all values the same, therefore it is not necessary to use newtons here.
	Raw: The drag force produced measured in grams.	
	Processed: The lift force to drag force ratio.	
Control	Airfoil dimensions other than maximum thickness.	Any variables other than the maximum thickness of the airfoils were kept constant for all the airfoils. These include the max camber, camber position, and thickness positions. Only the last two digits which represent the thickness varied between the airfoil NACA numbers.
	Wing Area	*Equations 3 and 4* highlight that the wing area A impacts the lift and drag forces. The width of all the airfoils was 6 cm and their length was 8 cm. The wing area is not the total surface area of a wing but rather the area looking down from above

		the wing; it is a projected area (Benson, n.d.). Therefore, the wing area for all six airfoils is 48 cm^2.
	Airspeed	The lift and drag equations, *Equations 3 and 4*, both contain v^2 therefore airspeed affects both the lift and drag produced. To keep the airspeed constant, the hairdryer was kept at a fixed distance from the airfoils. However, as the angle of attack changes the airfoil moves slightly away from the hairdryer. Therefore, to minimize any changes in airspeed the hairdryer was placed close to the airfoils, a distance of 2 cm away.
	Air Density	Air density is another quantity found in both the lift and drag equations. To keep air density the same for all trials, they were all conducted at the same altitude – same table, and the temperature of the room was kept within 3 °C for all trials.

Apparatus

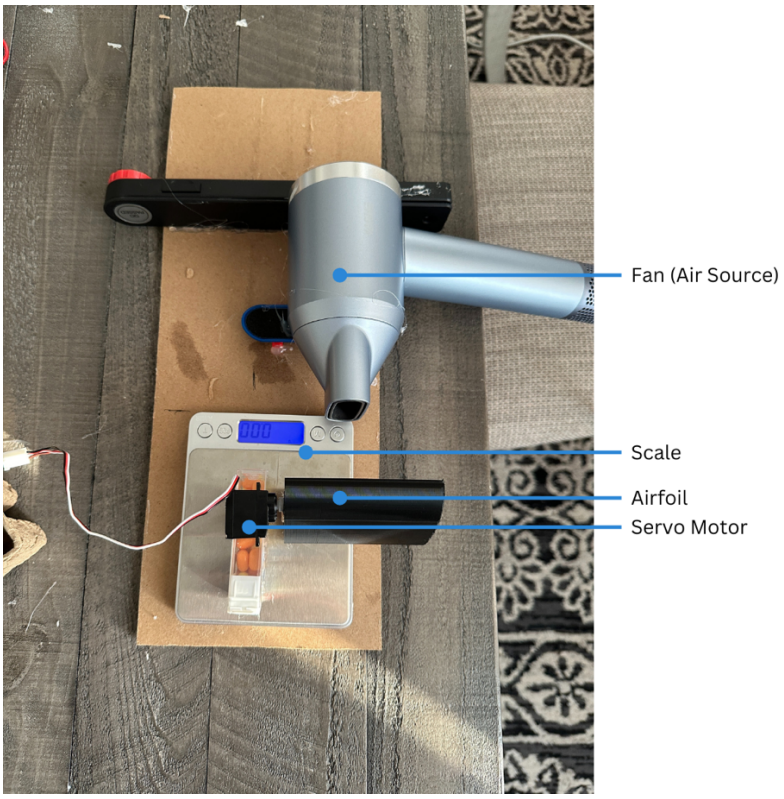

Figure 6: Labelled diagram of the lift apparatus

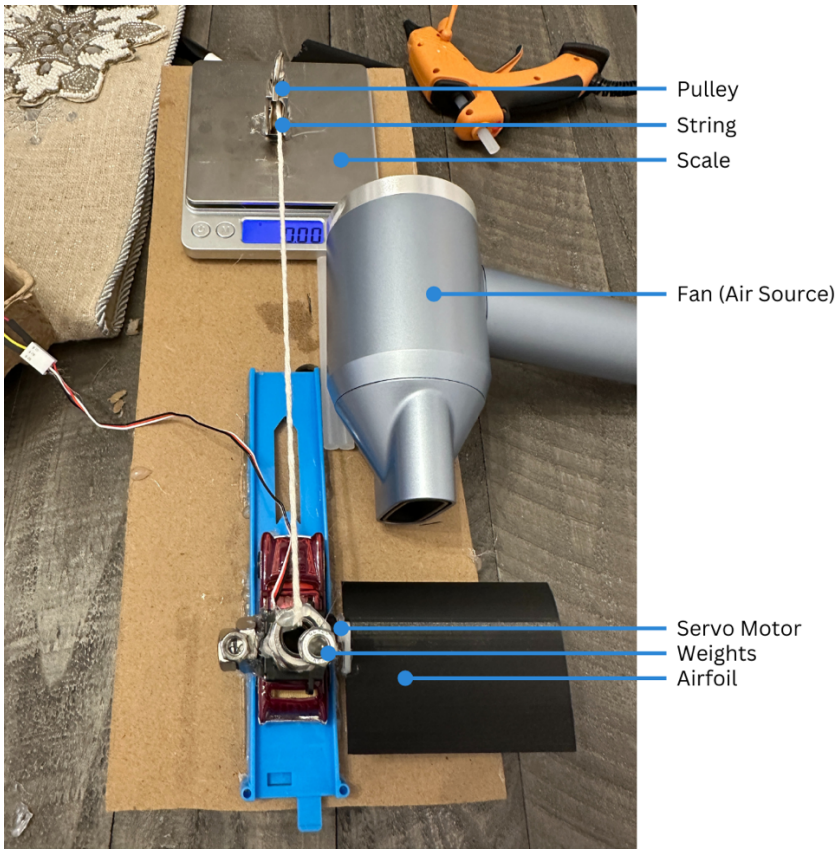

Figure 7: Labelled diagram of the drag apparatus

The entire drag apparatus was inclined by 3° to help the cart overcome its static friction. Since the scale was initially zeroed, this should not impact the values in any way. Weights were used to prevent the cart from tipping and to equalize the cart's weight for all six airfoils.

Procedure

Lift Analysis Procedure

1. The angle of the servo motor was set to 0°, then airfoil 5306 was mounted onto the servo motor. The balance was zeroed. The servo motor was then set to -5°.

    a. For each trial, the servo was initially set to 0° so that the airfoil was mounted with correct orientation.
2. The hairdryer was turned on giving it 5 seconds to accelerate to its final speed. The lift force was measured in grams after allowing the scale to settle on a value. The value was recorded in a spreadsheet.
    a. Since the balance gave a negative number for upward values, the record value was multiplied by -1.
3. Steps 1-2 were repeated incrementing the angle of attack by 5° until 60°.
4. Steps 1-3 were repeated for 4 more trials.
5. Steps 1-4 were repeated for the remaining 5 airfoils.

The drag procedure differed only in that after step four, when mounting a different airfoil, bolts were added to the cart to ensure that its weight remained relatively the same. This served to minimize the difference in static friction between the airfoils.

Safety

There were no safety concerns with physical contact. Caution was taken when handling hot devices such as the hot glue gun and 3d printer.

Data Analysis

Qualitative Results

At higher angles of attack, the wing became less stable and would vibrate more.

Quantitative Results

Data Analysis

Table 2: The Average Lift and Drag Forces Produced at Varying Angles of Attack

	Angle of Attack (± 1°)													
	-5	0	5	10	15	20	25	30	35	40	45	50	55	60
Airfoil	Lift Force (g)													
5306	-3.04	-1.68	-0.21	1.47	3.18	4.71	5.89	6.75	7.09	6.11	4.45	3.28	2.44	1.75
5309	-2.80	-1.50	0.13	1.72	3.41	4.94	6.25	7.05	7.32	6.55	4.23	3.17	2.45	1.74
5312	-3.04	-1.56	0.20	1.90	3.76	5.51	6.73	7.55	7.58	6.24	4.41	3.43	2.78	2.41
5315	-2.80	-1.08	0.57	2.52	4.68	6.59	8.13	9.26	9.70	8.44	6.18	4.85	4.01	3.16
5318	-2.85	-0.92	0.95	2.97	5.29	7.38	9.55	11.02	11.91	10.69	8.56	7.31	6.86	6.09
5321	-1.74	0.19	2.42	4.38	6.71	8.97	11.34	13.19	13.96	13.15	11.11	9.74	8.78	7.83
Airfoil	Drag Force (g)													
5306	0.24	0.19	0.16	0.15	0.20	0.32	0.50	0.82	1.14	1.66	2.13	2.39	2.70	3.13
5309	0.19	0.17	0.16	0.18	0.27	0.41	0.62	0.95	1.29	1.81	2.15	2.55	2.80	3.06
5312	0.27	0.21	0.18	0.20	0.24	0.33	0.47	0.76	1.06	1.51	1.89	2.31	2.80	3.21
5315	0.29	0.25	0.14	0.18	0.23	0.35	0.71	0.94	1.18	1.90	2.47	2.82	3.21	3.64
5318	0.35	0.34	0.32	0.25	0.30	0.41	0.57	0.78	1.08	1.45	2.16	2.32	2.82	3.42
5321	0.31	0.28	0.29	0.31	0.30	0.40	0.62	0.93	1.28	1.62	2.35	2.93	3.21	3.70

The uncertainty of the lift and drag forces were taken as the larger between the reading error of 0.01 g and $\frac{Trial_{max}-Trial_{min}}{2}$.

Table 3: The Lift to Drag Force Ratios Produced at Varying Angles of Attack

	Angle of Attack (± 1°)													
Airfoil	-5	0	5	10	15	20	25	30	35	40	45	50	55	60
5306	-12.67	-9.00	-1.36	9.80	15.88	14.87	11.70	8.23	6.23	3.69	2.09	1.37	0.91	0.56
5309	-14.48	-8.63	0.79	9.57	12.80	11.94	10.02	7.40	5.69	3.62	1.97	1.24	0.87	0.57

5312	-11.27	-7.43	1.09	9.48	15.65	16.69	14.31	9.93	7.15	4.14	2.34	1.49	0.99	0.75
5315	-9.67	-4.33	3.95	14.26	20.04	18.83	11.50	9.85	8.24	4.44	2.50	1.72	1.25	0.87
5318	-8.08	-2.69	2.96	12.05	17.44	18.01	16.85	14.07	10.99	7.35	3.97	3.15	2.43	1.78
5321	-5.67	0.68	8.25	13.99	22.63	22.43	18.30	14.13	10.94	8.10	4.73	3.33	2.74	2.12

Lift to Drag Ratio Calculation	Uncertainty
L/D = -3.04 g / 0.24 g L/D = -12.67	Fractional uncertainty = $\frac{0.045}{3.04} + \frac{0.065}{0.24}$ Fractional uncertainty = 0.2856 Absolute Uncertainty = 0.2856 * -12.67 Absolute Uncertainty = 3.62 Absolute Uncertainty = 4

Graph Analysis

Lift

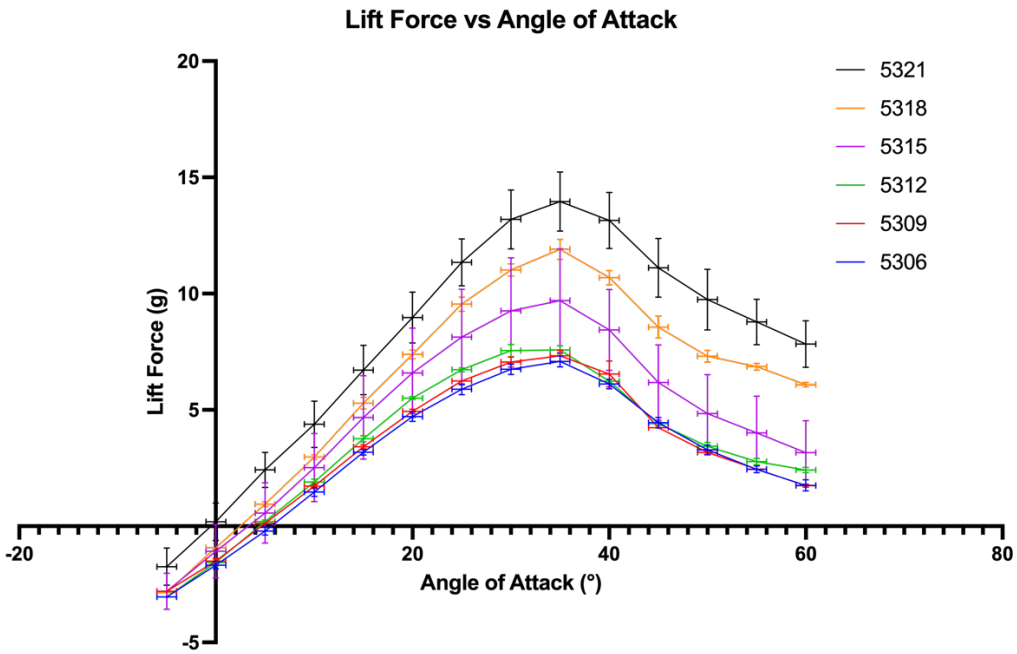

Figure 8: Lift force according to angle of attack.

The graph in figure 8 highlights a common shape for all the airfoils; all curves show an increase in lift until a critical angle then the lift force begins to decrease. All airfoils present the same critical angle of at least 35° and less than 40° as the graph is interpolated between these points. The lift force increases fairly linearly between 0° and 30°, then there is a parabolic decrease in lift. In the linear portion, between 0° and about 25°, the increase in lift for thicker airfoils is much smaller than after 25°; the lines are more condensed in the linear portion.

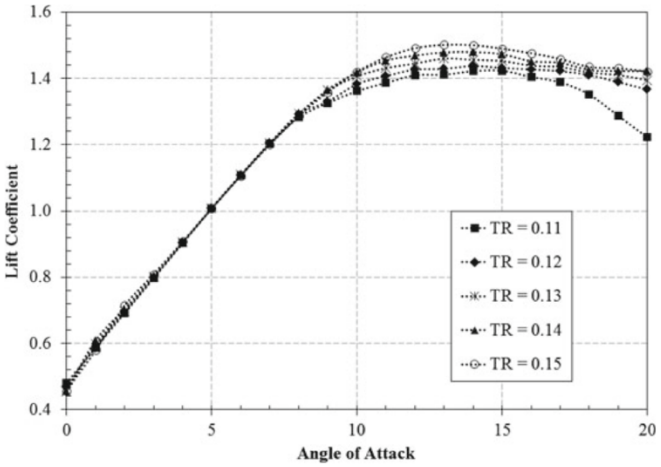

Figure 9: Lift force according to angle of attack from a literature source. TR is the ratio of maximum thickness to the chord length. The curves show airfoils 4411-4415. (Roy et al., 2021)

Figure 9 shows the lift curves for 5 airfoils of different thickness according to a different literature source. The relationship found in this procedure is similar to that of the literature work. However, the literature values shows that all airfoils produce the same lift force during the linear portion. This could be attributed to the fact that the literature source varied the thickness through a much smaller ranger of 11% to 15% of the chord while this procedure varied it throughout 6 to 21% of the chord.

After the linear portion, the curves show an exponential relationship between airfoil thickness and the lift produced: airfoils 5306 and 5309 are very close together and even overlap slightly, while airfoil 5321 generates a much higher lift force than airfoil 5318 during the curved portion. This can be seen by plotting the lift produced at the critical angle of 35°.

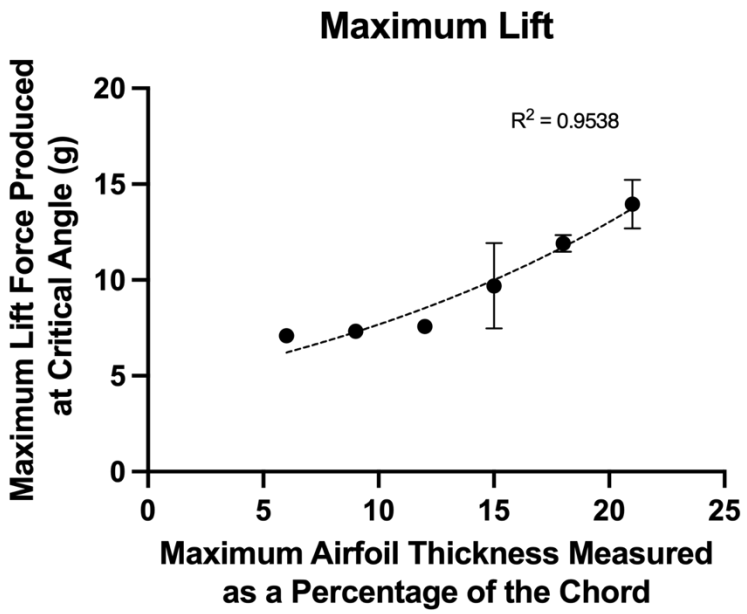

Figure 10: The maximum lift force produced – the lift force at the critical angle – according to airfoil thickness.

Figure 10 shows that the lift force is exponentially related to the maximum airfoil thickness for high angles of attack, having a high R^2 value of 0.9538. This relationship deviates from the literature source which highlights a linear relationship between airfoil thickness and lift force, during the curved portion. This could once again be a cause of the difference in range between airfoil thickness. Alternatively, it could be due to the difference in max camber and max camber position, which are the first two digits of the airfoil NACA numbers. The literature value had a max camber of 4% of the chord located 40% from the leading edge, while this procedure used 5% and 30% respectively.

Drag

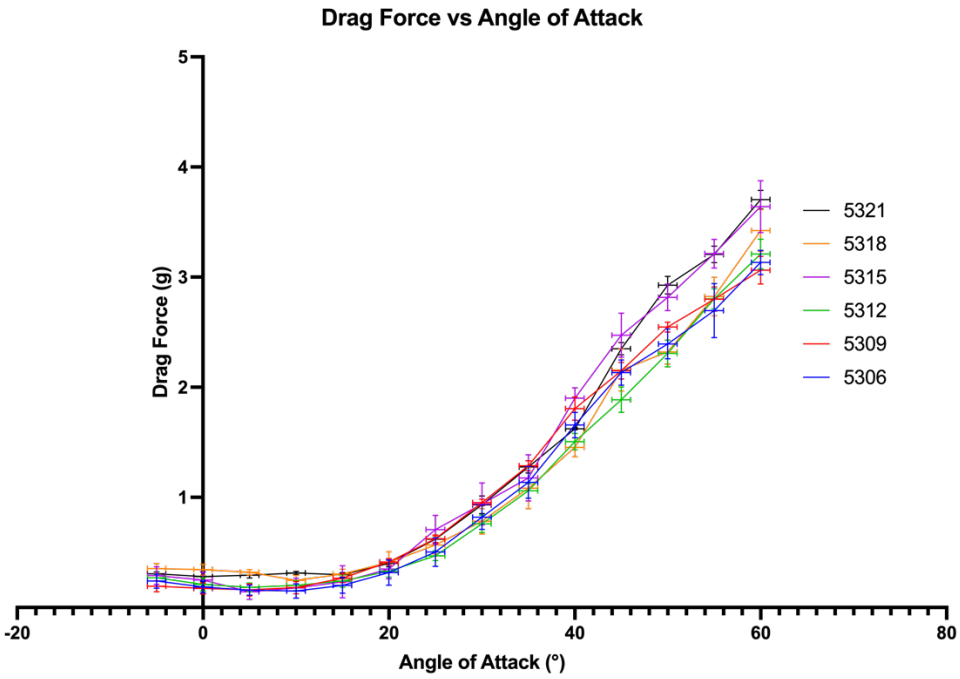

Figure 11: Drag force according to angle of attack.

Figure 11 highlights the relationship between the drag force and the angle of attack for the 6 airfoils tested. The relationship is not as clear as that for the lift force which indicates high uncertainty. All airfoils show an exponential relationship between drag and angle of attack. The general trend appears to be that the thinner airfoils produce lower drag values for all angles of attack. This could be explained with the types of drag forces. Since the lift force increases with airfoil thickness, particularly at high angles of attack (Figures 8 and 10), thicker airfoils must also produce more induced drag by *Equation 5*. As well, thicker airfoils also produce more parasitic drag due to a larger surface area.

That being said, the graph is not clear enough to determine if the relationship between airfoil thickness and drag force is exponential like for the lift force. However, there is some indication that the curves are closer together for lower angles of attack and diverge for higher ones.

Lift to Drag Ratio

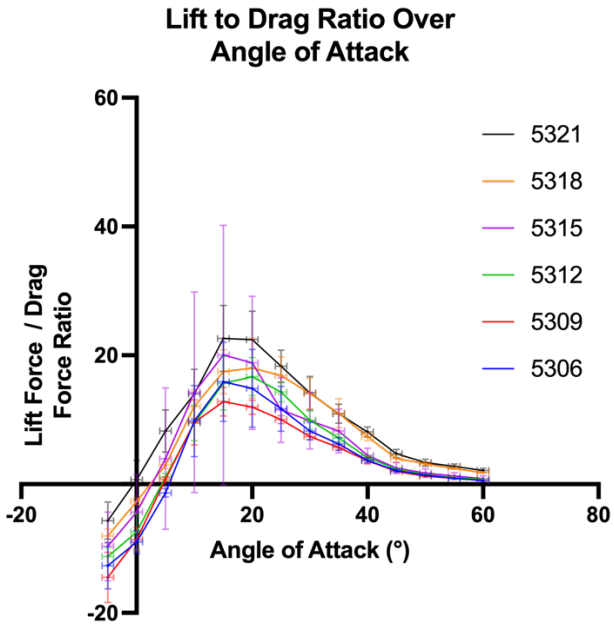

Figure 12: Lift to drag ratio according to angle of attack.

In Figure 12, it is seen that for all airfoils, the L/D ratio rises linearly, peaks, then falls in a parabolic fashion. The curves become very condensed in the downward parabolic portion. The peak L/D ratio occurs between 15° and 20° for all the airfoils.

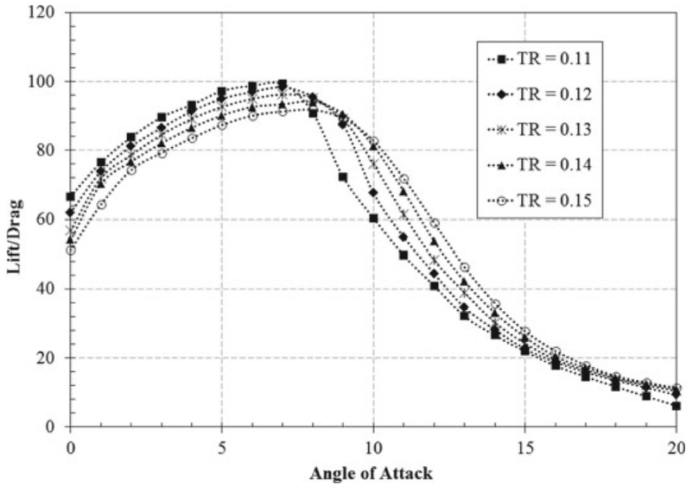

Figure 13: Lift to drag ratio according to angle of attack from a literature source. (Roy et al., 2021)

Figure 13 highlights the relationship obtained in the literature source between L/D ratio and airfoil thickness. This figure shows that after the peak L/D ratio, the relationship between airfoil thickness and L/D ratio acts the same as in Figure 12. Before the peak L/D ratio however, thinner airfoils have higher L/D ratios. This relationship is not present from the data obtained in this procedure. An explanation for this could be that the drag values obtained in this procedure are too faint to show a reversing relationship. Table 2 shows that the maximum average lift force was 13.96 g while the maximum average drag force was 3.70 g. Alternatively, it could be that differing relationships are seen at low angles of attack due to differences in parasitic drag. At low angles of attack, with less lift produced, parasitic drag likely has a largely portion of the total drag force than at high angles of attack with more induced drag. Thus, it may be that the different constant conditions used, max camber and camber position, and the difference in the range of the independent variable influenced the parasitic drag between this procedure and the literature source.

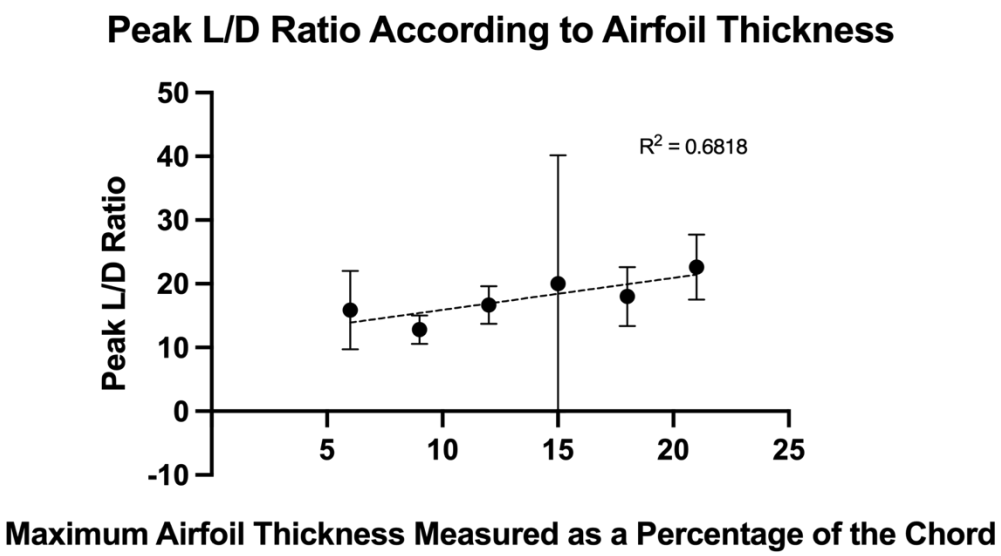

Figure 14: The maximum lift to drag ratio according to airfoil thickness.

The relationship between peak L/D ratio and airfoil thickness is linear. Peak L/D ratio has a medium correlation with the airfoil thickness, $R^2 = 0.6818$. Since the lift force seems to increase faster than drag force for thicker airfoils, the net effect is a linear increase in the L/D ratio.

Conclusion

The initially proposed hypothesis was correct. It successfully predicted that thicker airfoils would produce a higher lift and drag force at every angle of attack. However, it failed to predict that changing the thickness of an airfoil would not affect the critical angle and that lift would grow faster than drag with thicker airfoils, especially at higher angles of attack which is also supported by a literature source. The relationship between drag force and airfoil thickness is also not clearly defined through this procedure.

Addressing the research question, **"How does an airfoil's maximum thickness affect the lift versus drag produced at various angles of attack?"**, this procedure showed that airfoil thickness increases both the lift and drag forces produced at all angles of attack. The lift forces increase at a greater rate, however, leading to a linear relationship between airfoil thickness and the L/D ratio.

As mentioned earlier, a higher L/D ratio means a shallower flight path which is a necessity for gliders which lack an onboard propulsion system and that must trade altitude for airspeed to produce a lift force. Aircraft with propulsion systems that want to maximize lift producing capabilities, should opt for thicker airfoils, while those that seek to minimize drag forces should have thinner airfoils although this comes with a loss in L/D ratio.

There was some divergence from literature sources. Further research is needed to determine the reliability of this experiment. Specifically, in determining how the constant factors affect the relationship between airfoil thickness and lift/drag forces.

Evaluation

A large contributor to error in this experiment was the fluctuations in the fluid flow. The hairdryer used to generate the airstream likely experienced wear over time, potentially preventing it from producing the same air temperature and speed over time. Additionally, the procedure was carried out over multiple days, with varying room temperature. Both the air density and the airspeed affect the lift and drag forces produced by an airfoil, *Equations 3 and 4*. Higher air density and airspeed lead to higher lift and drag forces. This random error could be

reduced by conducting all trials within a smaller time frame, in a better temperature-controlled environment, and using a better airstream source.

Another contributor to error was the method used to change the angle of attack of the airfoils The airfoils were supported only on one side by a servo motor which was used to alter their angle. For this reason, an uncertainty of ± 1° was given to the angle of attack measurements. With thicker airfoils, the servo motor was forced to support more weight which caused the airfoils to buckle slightly. This meant the angle of attack varied between the right and left sides of the airfoil. This error could be eliminated by supporting the airfoils from both sides.

There is also large uncertainty in raw values which is seen in the error bars of graphs. To combat this, more precise measuring tools could be used in recording data. Specifically, a more precise scale could have helped to reduce the error bars.

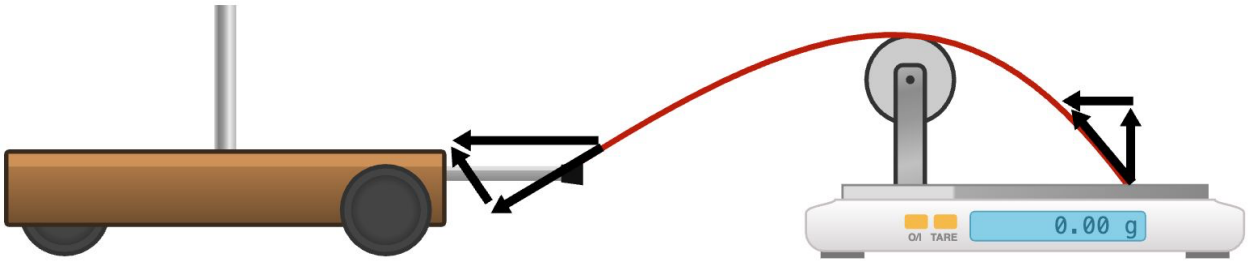

Figure 15: Force transfer within the drag apparatus from Figure 7.

Furthermore, the drag forces showed great fluctuation, and a clear pattern was not developed. This was likely due to the apparatus used to measure drag. The cart had friction with the ground which had to be overcome by the drag force. To equalize this impact, weights were added to the cart to allow it to have a similar weight for each airfoil. However, the weights could not be added

in fine instruments and so there was still much variation in the cart's weight during the trials of different airfoils. Also, as the airfoils were mounted only from one side, airfoils that produced more drag tended to divert the cart to one side of the track causing even more friction. As well, since the rope connecting the scale and cart was not mounted at perfect angles, a smaller amount of the force acted on the scale. This likely contributed to the faintness of the drag forces, which in turn may have been the differentiating factor between this procedure's L/D ratios and the literature source's ones.